



## High resolution imaging for subtle geological features in the Llanos basin

\*Michael Smith, Geotrace; Paul Cunningham, Amigos Energy Advisors L.L.C.; David Behrman, Amigos Energy Advisors L.L.C.

Copyright 2011, SBGf - Sociedade Brasileira de Geofísica

This paper was prepared for presentation during the 12<sup>th</sup> International Congress of the Brazilian Geophysical Society held in Rio de Janeiro, Brazil, August 15-18, 2011.

Contents of this paper were reviewed by the Technical Committee of the 12<sup>th</sup> International Congress of the Brazilian Geophysical Society and do not necessarily represent any position of the SBGf, its officers or members. Electronic reproduction or storage of any part of this paper for commercial purposes without the written consent of the Brazilian Geophysical Society is prohibited.

### Abstract

We demonstrate in a seismic processing project from the Llanos basin in Colombia that increasing bandwidth prior to migration can improve the spatial (lateral and vertical) resolution and the subsequent velocity analysis can produce a more detailed velocity profile which in turn improves image quality. The increase in bandwidth prior to migration reduces both vertical and lateral wavelet widths and, thus, increases spatial resolution. The improved spatial resolution in turn permits a more detailed velocity field to be defined both laterally and vertically. This approach, bandwidth expansion prior to migration, can be applied to both time and depth migration flows.

We apply the high resolution imaging technique to the relatively thin Oligocene to Early Miocene Carbonera sandstones from the Llanos basin. Traps are typically three-way structural closures bounded by faults with relatively small throws. Using the high-resolution imaging, the thin sands, their lateral pinchouts and the fault locations can be more accurately mapped reducing exploration risk.

### Introduction

Resolution, in seismic imaging, relates to the ability to distinguish closely spaced events. Two main factors affecting resolution are the width of the main lobe of the wavelet and side lobe energy in relation to the main lobe. Side lobes become a problem when the bandwidth of the wavelet is less than 1.5 - 2 octaves (Kallweit and Wood 1982). Other factors affecting resolution in seismic imaging include aperture, noise, velocity model, migration algorithm, and coarse sampling

The theoretical maximum resolution is rarely achieved due to the factors noted above. This work focuses on what Vermeer (1999) referred to as achievable resolution, generally understood as the best possible resolution given the above constraints.

One of the most difficult constraints to overcome is the available bandwidth which is often less than what is needed to properly image the data. This is due to the non-elastic nature and heterogeneities of the subsurface that result in a dissipation of high frequency signal (conversion to heat) and velocity dispersion. These effects distort and

stretch the wavelet, lowering the resolution of our seismic data (Wang, 2006). Ideally we would like to reverse some of these effects and increase our bandwidth available for migration.

To address this limitation we use an algorithm which recovers some of the lost wavelet characteristics. The algorithm uses the available bandwidth of the fundamental frequencies to compute harmonics and adds them back into the wavelet by a convolution-like process in the CWT domain. This reshapes the wavelet and broadens the available bandwidth in the seismic data (Smith et al. 2008).

### Theory

Vermeer (1999), using Belkyin's formula, and Kallweit and Wood (1982) zero phase wavelet work, derived a set of equations for resolution of both 2D zero-offset data and 2D offset planes for constant velocity media.

$$R_x = \frac{cv}{2 \sin \theta_{x \max} f_{\max}} \quad (1)$$

$$R_z = \frac{cv}{2 f_{\max}} \quad (2)$$

$$R_x = \frac{cv}{2 \sin \theta_{x \max} f_{\max} \cos i} \quad (3)$$

$$R_z = \frac{cv}{2 f_{\max} \cos i} \quad (4)$$

Equations 1 and 2 are the lateral and vertical resolution for zero offset data, whereas equations 3 and 4 are for 2D offset planes. The  $c$  term is the correction for wavelet width (Kallweit and Wood 1982),  $v$  is velocity,  $\theta_{x \max}$  is the maximum dip angle imaged by the aperture radius (Figure 1),  $f_{\max}$  the maximum available frequency and  $\cos i$  is the cosine of the incident angle  $i$ .

From Equation 1 we see that lateral resolution is dependent on both aperture and frequency. It follows that resolution increases with the sine of the dip angle imaged by the aperture radius and that resolution increases with increasing frequency. In fact, resolution doubles with each octave increase in frequency (Figure 2). Equation 3 has an additional term which decreases resolution with increasing incidence angle. This comes from migration stretch (NMO stretch). This simply means that as the offsets increase the resolution decreases due to the stretching of the wavelet.

From Figure 2 we see that when the aperture to depth ratio exceeds 1 (about 45 degrees for  $\theta_{x_{max}}$ ) there is a small increase in resolution. However, we continue to achieve a doubling of resolution for every octave increase in maximum available frequency.

Up to this point all of the equations and examples have addressed 2D resolution. The resolution of 3D data (the 3D spatial wavelet) can be obtained as the normalized sum of all of the contributing 2D spatial wavelets (Vermeer 1999).

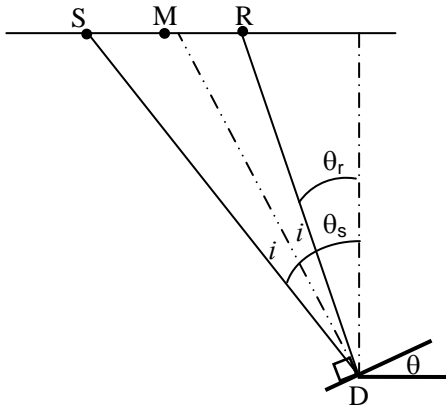


**Figure 1** Diagram of a diffractor  $D$  illuminated by the source/receiver pair  $S/R$  with dip angle of  $\theta = (\theta_s + \theta_r)/2$  with ray path having an incident angle  $i = (\theta_s - \theta_r)/2$ .

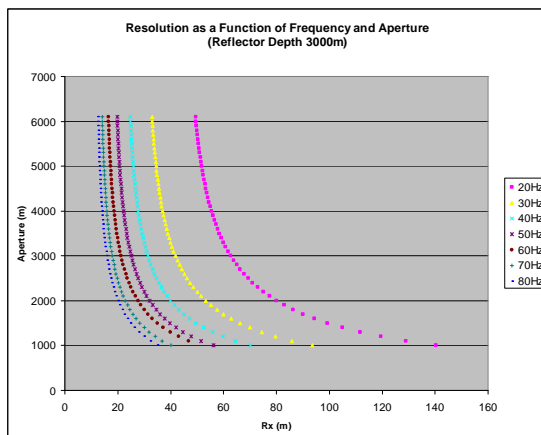


**Figure 2** Plot showing lateral resolution  $R_x$  for constant frequencies and varying apertures. Note how the resolution doubles for every octave increase in frequency.

### Application

The Llanos basin is a modern day savannah region characterized as a Cenozoic foreland basin located in eastern Colombia. It is bounded on the west side by the Guaicaramo – Yopal fault system associated with the Eastern Cordillera of the Andes, to the east by the Guyana shield and to the south by the Macarena high and Vaupés Arch

The 3D seismic area is located in the Casanare Department on trend with numerous discoveries made

within the past decade. The typical stratigraphic column for this area is characterized by Late Cretaceous and Tertiary deposits associated with the subsidence of the Llanos basin in response to Andean Cordillera uplift to the west. The Carbonera sequence, the primary target of this seismic project, is the result of four major marine-influenced, lower coastal plain deposition cycles during the Oligocene to Early Miocene (Cooper et al., 1995). It overlays a Cretaceous to Eocene sequence containing secondary exploration targets such as the Une and Guacheta sandstones and the Gacheta shale which, in the western (deeper) edge of the basin, is the primary source rock.

Most exploration drilling to date has been focused on three-way structural closures bounded by normal, up-to-the-basin faults. Much of the normal faulting is thought to be due to flexure of the basin due to increased load of the Andean cordilleras. These faults often have small throws (5 to 25 meters) which, despite their size, are sufficient to provide a seal. However, because of poor resolution they are not always easily mapped accurately on seismic data.

### Results

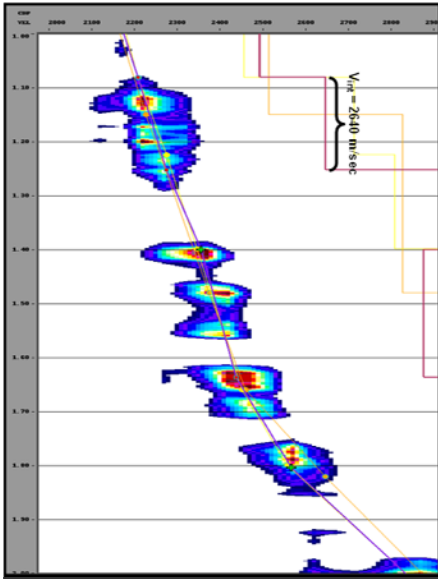
In Figures 3 and 4, we see the velocity panels obtained for a common image gather in the conventional migration and broadband imaging. In figure 4 the velocity function is overlaid from figure 3 and it can be seen that the lower frequency function appears as an average of the higher frequency function. The lower frequencies are acting as a low pass filter and smoothing the velocity function. With higher frequency velocity fields we can better position the image relative to the lower frequency velocity functions.

Figure 5 compares the spectral characteristics of the conventional pre-stack time migration with the extended bandwidth migration over the interval of interest of 1-2 seconds two-way time. We see an increase of nearly an octave of bandwidth in the extended versus the conventional migration.

In Figures 6 and 7, we see a comparison of the clarity with which faults can be better delineated on the high resolution imaged data when compared with a conventional pre-stack time migrated section.

An example of the subtle stratigraphic features that are seen on the high resolution imaging, but not in the conventional pre-stack time migration, are shown in Figures 8 and 9.

Another interesting feature is that the high resolution migration data has laterally moved subtle structures. Some wells that were drilled on ostensible structural highs based on the interpretation of conventional pre-stack time migrated data turned out not to be on the actual structural apex as later confirmed by drilling results. While not yet tested, the lateral shifts of these structures in the direction of the actual structural high leads us to believe that one of the benefits of high resolution migration is greater possible accuracy in the positioning of seismic features. An example is shown in Figures 9 and 10 where the structural high shifted eastwards by approximately 100 meters from Figure 10 as seen on Figure 11.



**Figure 3** Conventional pre-stack time migration velocity panel with RMS velocity function and interval velocities shown. Interval velocity highlighted is 2640 m/s.

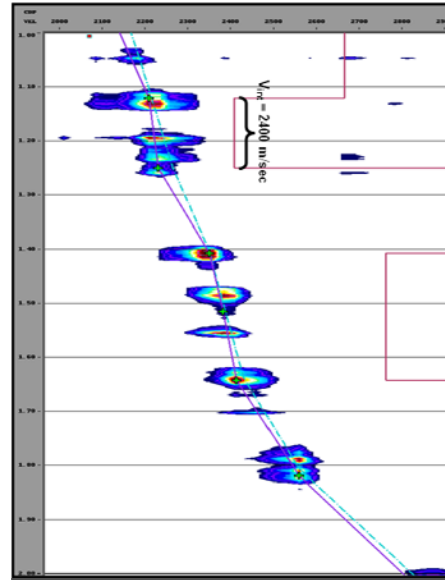


**Figure 4** Extended bandwidth imaging migration velocity panel with RMS velocity function and interval velocities shown. The blue dashed line is the RMS velocity function from the conventional migration. Interval velocity highlighted is 2400 m/s.

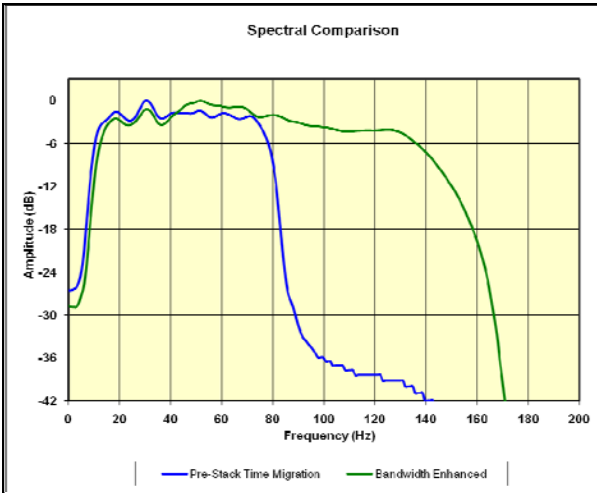


**Figure 5** Spectral comparison of pre-stack time migrated volume versus high-resolution volume.

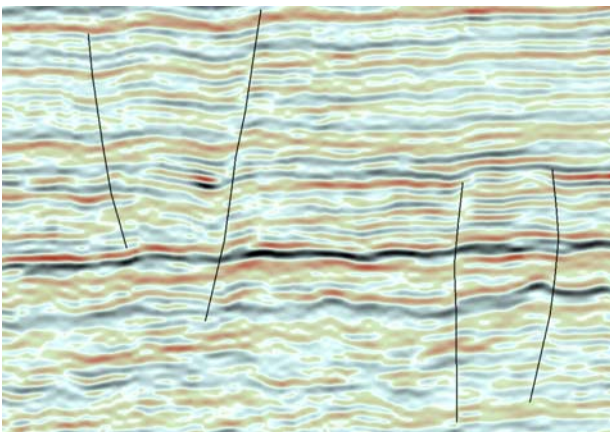


**Figure 6** Conventional pre-stack time migration with fault picks from the extended bandwidth imaging interpretation.

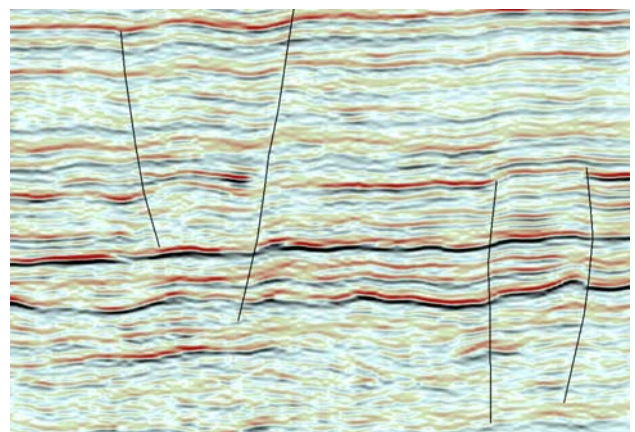


**Figure 7** Extended bandwidth imaging with fault picks showing sharpened fault imaging.

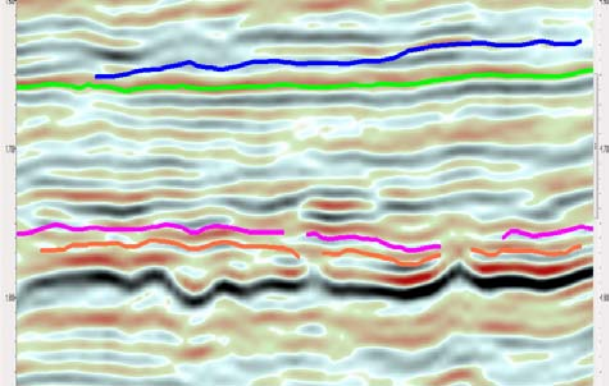


**Figure 8** Conventional pre-stack time migration with stratigraphic interpretation from extended bandwidth imaging.

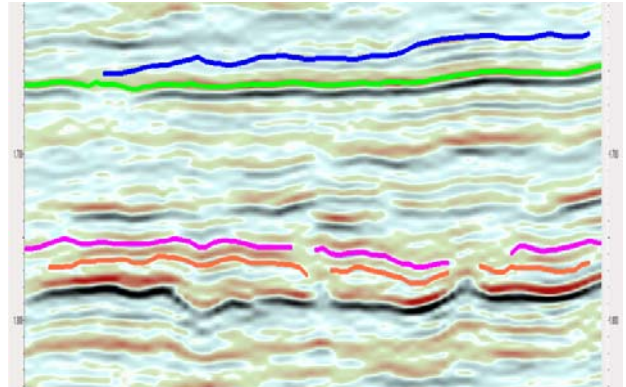


**Figure 9** Extended bandwidth imaging with stratigraphic interpretation.

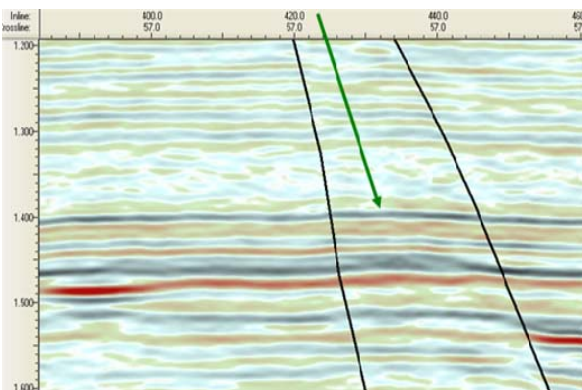


**Figure 10** Conventional pre-stack time migration with arrow showing structural high.

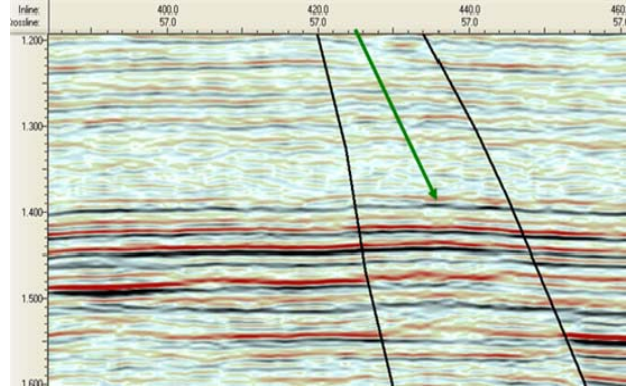


**Figure 11** Extended bandwidth imaging with arrow showing structural high moved by 100 meters in correct direction.

## Conclusions

Vermeer (1999) derived equations for 2D spatial resolution (3D spatial resolution is just the normalized sum of the contributing 2D spatial resolutions) that are for constant velocity but are sufficient for first order approximations of spatial resolution. These equations show us that aperture and frequency are key components in spatial resolution after migration.

We have shown that by increasing bandwidth prior to migration the expected uplift is present on the data after migration. This comes from both an extension of frequency, but also a higher resolution velocity function can be built both in the vertical and lateral directions. Additionally, an additional application of bandwidth extension can be done to mitigate against migration stretch.

The application of high resolution imaging on the Llanos basin data has enabled an improved interpretation of the seismic including reducing the uncertainty in locating minor faults, providing a better understanding of the stratigraphic aspects of the section and sharper delineation of target reservoir zones.

## Acknowledgments

The authors would like to thank John Sharry of Amigos Energy Advisors L.L.C., for helpful review and comments, and thank Geotrace for permission to submit this paper.

## References

- Cooper, M. A., Addison, F. T., Alvarez, R., Coral, M., Graham, R. H., Hayward, A. B., Howe, S., Martinez, J., Naar, J., Peñas, R., Pulham, A.J., Taborda, A. [1995] Basin Development and Tectonic History of the Llanos Basin, Eastern Cordillera, and Middle Magdalena Valley, Colombia: AAPG Bulletin, **79**, No. 10, 1421-1443
- Kallweit, R. S., and Wood, L. C. [1982] The limits of resolution of zero-phase wavelets: Geophysics, **47**, 1035-1046
- Smith, M., Perry, G., Stein, J., Bertrand, A., Yu, G. [2008] Extending seismic bandwidth using the continuous wavelet transform: First Break, **26**, 97-102.
- Vermeer, G. J. O. [1999] Factors effecting spatial resolution: Geophysics, **64**, 942-953
- Wang, Y. [2006] Inverse Q-filter for seismic resolution enhancement: Geophysics, **71**, 51-60